Supplemental Table 1. Statistics of X-ray diffraction and structure refinement [a]

	Native	Pt SAD	S SAD
Data collection statistics			
Space group	$P4_32_12$	$P4_32_12$	$P4_32_12$
$\alpha, \beta, \gamma, °$	90, 90, 90	90, 90, 90	90, 90, 90
Unit cell (a, b, c), Å	174.7, 174.7, 104.6	173.8, 173.8, 104.6	174.5, 174.5, 104.7
Resolution range (Å)	50.0-2.50 (2.56-2.50) [b]	50.0-3.50 (3.59-3.50)	50.0-3.30 (3.39-3.30)
Completeness (%)	98.7 (87.2)	99.9 (100.0)	99.9 (100.0)
Number unique reflections	55,726 (3,570)	38,576 (2,865)	46,450 (3,464)
Redundancy	14.1 (10.9)	15.6 (15.8)	13.4 (13.4)
R_{merge} (%) [c]	15.5 (519)	15.9 (135)	10.9 (57.7)
$I/\sigma(I)$	13.3 (0.41)	16.3 (2.99)	21.6 (5.35)
$CC_{½}$ (%) [d]	99.9 (11.4)	99.9 (86.6)	99.9 (95.1)
Wavelength (Å)	0.97931	1.06975	1.90745
Refinement statistics			
R_{work} (%) [e]	19.9 (37.1)		
R_{free} (%)	24.2 (38.5)		
Bond RMSD (Å)	0.005		
Angle RMSD (°)	0.71		
Ramachandran plot [f] (Favored/allowed/outlier)	95.6/4.2/0.2		
Number of atoms			
Protein	7273		
Ligand	87		
Water	100		
B factor			
Protein	101.3		
Ligand	140.2		
Water	82.9		
Molprobity percentile (Clash/Geometry)	99/99		
PDB	6N29		

a. Anomalous data was collected at 1.06975 Å for platinum SAD and at 1.90745 for sulfur SAD. Only the 1.06975 Å data was strong enough to be useful for phasing or refinement. However, the 1.90745 data was useful for confirming locations of sulfurs in disulfide bonds and the identity and location of the Ca ion as shown in Supplemental Fig. 3.

b. The numbers in parentheses refer to the highest resolution shell.

c. Rmerge = $\Sigma h \Sigma i |Ii(h) - \langle I(h) \rangle| / \Sigma h \Sigma i Ii(h)$, where Ii(h) and <I(h)> are the i^{th} and mean measurement of the intensity of reflection h.

d. Pearson's correlation coefficient between average intensities of random half-datasets for each unique reflection[1].

e. Rfactor = $\Sigma h||Fobs(h)|-|Fcalc(h)|| / \Sigma h|Fobs(h)|$, where Fobs (h) and F calc (h) are the observed and calculated structure factors, respectively. No $I/\sigma(I)$ cutoff was applied.

f. Calculated with MolProbity[2].

References.

1. Karplus PA, Diederichs K. Linking crystallographic model and data quality. *Science.* 2012;336(6084):1030-1033.

2. Davis IW, Leaver-Fay A, Chen VB, et al. MolProbity: all-atom contacts and structure validation for proteins and nucleic acids. *Nucleic Acids Res.* 2007;35:W375-383.

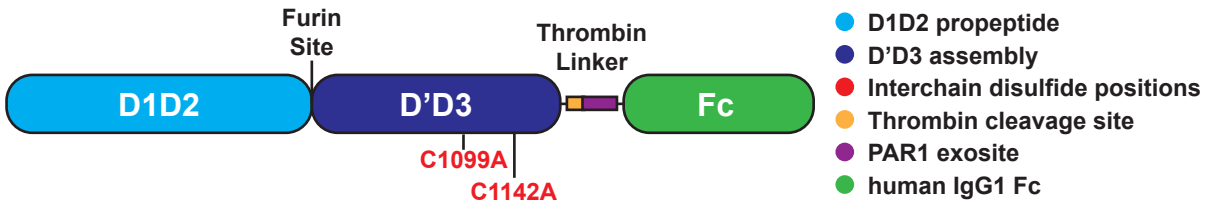


```
   1 MIPARFAGVL LALALILPGT LCAEGTRGRS STARCSLFGS DFVNTFDGSM YSFAGYCSYL
  61 LAGGCQKRSF SIIGDFQNGK RVSLSVYLGE FFDIHLFVNG TVTQGDQRVS MPYASKGLYL
 121 ETEAGYYKLS GEAYGFVARI DGSGNFQVLL SDRYFNKTCG LCGNFNIFAE DDFMTQEGTL
 181 TSDPYDFANS WALSSGEQWC ERASPPSSSC NISSGEMQKG LWEQCQLLKS TSVFARCHPL
 241 VDPEPFVALC EKTLCECAGG LECACPALLE YARTCAQEGM VLYGWTDHSA CSPVCPAGME
 301 YRQCVSPCAR TCQSLHINEM CQERCVDGCS CPEGQLLDEG LCVESTECPC VHSGKRYPPG
 361 TSLSRDCNTC ICRNSQWICS NEECPGECLV TGQSHFKSFD NRYFTFSGIC QYLLARDCQD
 421 HSFSIVIETV QCADDRDAVC TRSVTVRLPG LHNSLVKLKH GAGVAMDGQD IQLPLLKGDL
 481 RIQHTVTASV RLSYGEDLQM DWDGRGRLLV KLSPVYAGKT CGLCGNYNGN QGDDFLTPSG
 541 LAEPRVEDFG NAWKLHGDCQ DLQKQHSDPC ALNPRMTRFS EEACAVLTSP TFEACHRAVS
 601 PLPYLRNCRY DVCSCSDGRE CLCGALASYA AACAGRGVRV AWREPGRCEL NCPKGQVYLQ
 661 CGTPCNLTCR SLSYPDEECN EACLEGCFCP PGLYMDERGD CVPKAQCPCY YDGEIFQPED
 721 IFSDHHTMCY CEDGFMHCTM SGVPGSLLPD AVLSSPLSHR SKRSLSCRPP MVKLVCPADN
 781 LRAEGLECTK TCQNYDLECM SMGCVSGCLC PPGMVRHENR CVALERCPCF HQGKEYAPGE
 841 TVKIGCNTCV CRDRKWNCTD HVCDATCSTI GMAHYLTFDG LKYLFPGECQ YVLVQDYCGS
 901 NPGTFRILVG NKGCSHPSVK CKKRVTILVE GGEIELFDGE VNVKRPMKDE THFEVVESGR
 961 YIILLLGKAL SVVWDRHLSI SVVLKQTYQE KVCGLCGNFD GIQNNDLTSS NLQVEEDPVD
1021 FGNSWKVSSQ CADTRKVPLD SSPATCHNNI MKQTMVDSSC RILTSDVFQD CNKLVDPEPY
1081 LDVCIYDTCS CESIGDCAAF CDTIAAYAHV CAQHGKVVTW RTATLCPQSC EERNLRENGY
1141 EAEWRYNSCA PACQVTCQHP EPLACPVQCV EGCHAHCPPG KILDELLQTC VDPEDCPVCE
1201 VAGRRFASGK KVTLNPSDPE HCQICHCDVV NLTCEACQEP GGLVPRSFLL RNPNDKYEPF
1261 WEDEESDKTH TCPPCPAPEL LGGPSVFLFP PKPKDTLMIS RTPEVTCVVV DVSHEDPEVK
1321 FNWYVDGVEV HNAKTKPREE QYNSTYRVVS VLTVLHQDWL NGKEYKCKVS NKALPAPIEK
1381 TISKAKGQPR EPQVYTLPPS RDELTKNQVS LTCLVKGFYP SDIAVEWESN GQPENNYKTT
1441 PPVLDSDGSF FLYSKLTVDK SRWQQGNVFS CSVMHEALHN HYTQKSLSLS PGK
```

Supplemental Figure 1. Cartoon representation of the D1D2D'D3-Fc expression construct with its sequence below and colored according to the regions in the cartoon. The plasmid containing the construct, pSYN-VWF-039, has been deposited at AddGene (Watertown, MA) with ID 120292.

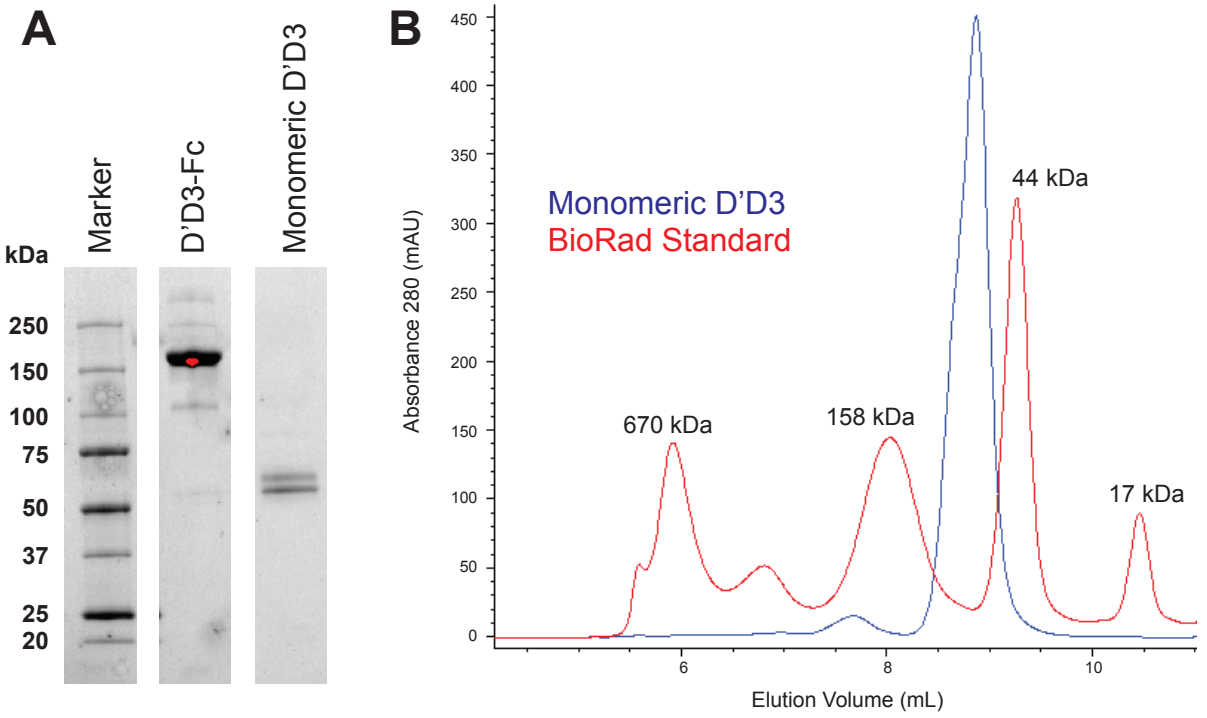

Supplemental Figure 2. A. Non-reducing SDS-PAGE showing purified D'D3-Fc prior to thrombin and Endo Hf cleavage and the final, thrombin and endo Hf-cleaved D'D3 monomer. B. The same D'D3 monomer was run on analytical size exclusion chromatography to confirm its purity and monomeric state. BioRad standard is shown for comparison.

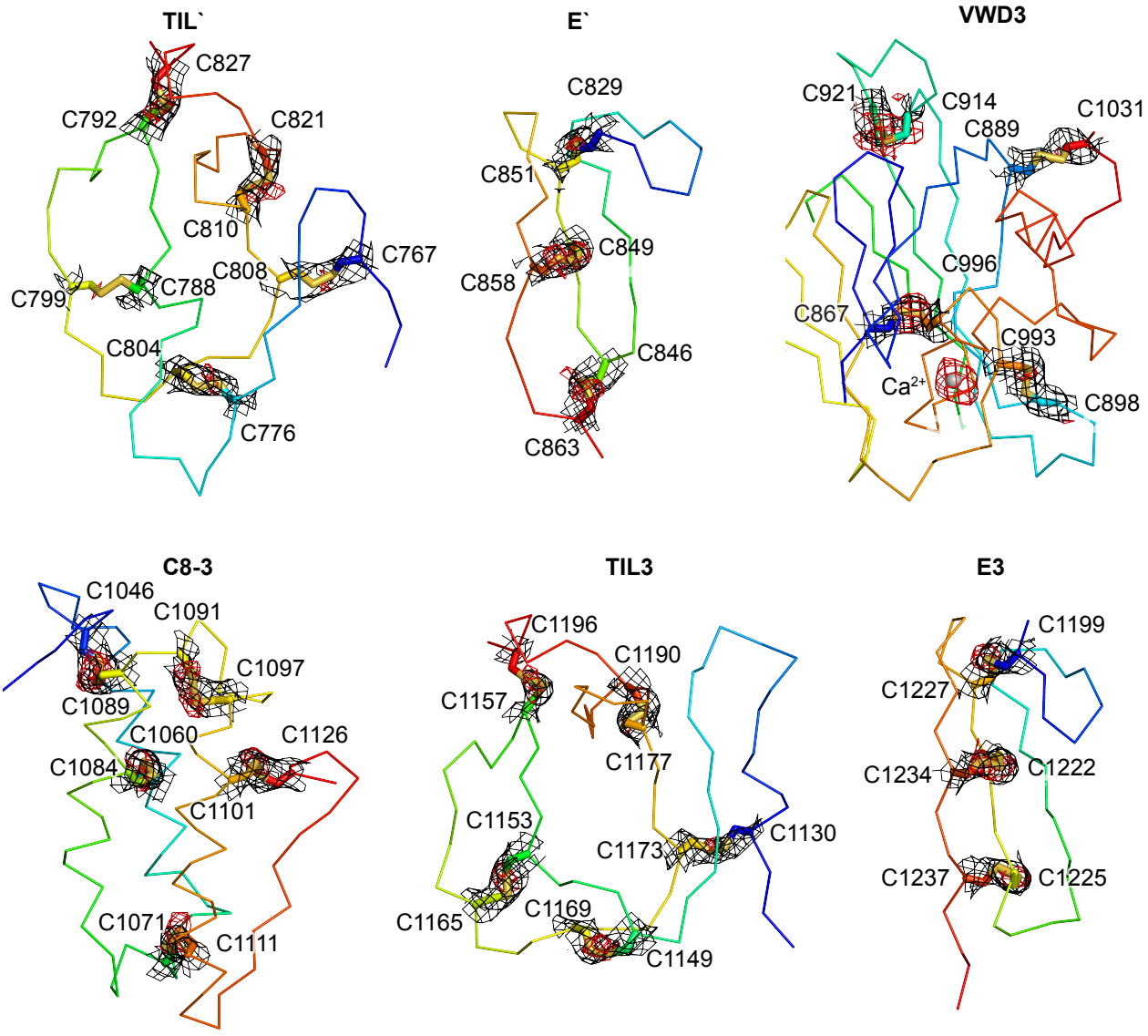

Supplemental Figure 3. Electron density around cysteine sulfurs and Ca^{2+} in D'D3. Anomalous difference maps from 1.9 Å-wavelength diffraction contoured at 3 σ (red mesh) and carved at 2 Å around cysteine residues and Ca^{2+} indicates the position of sulfur and calcium atoms. Composite omit simulated annealing maps contoured at 1 σ (black mesh) are similarly carved within 2 Å of cysteine residues. The densities confirm evidence for the disulfide bonds defined in the structure. The identity of the metal ion as Ca^{2+} is confirmed by the anomalous diffraction at 1.9 Å-wavelength, together with excellent agreement of the 2Fo-Fc maps from diffraction at 0.979 Å-wavelength with the density expected for Ca^{2+}, the metal-oxygen distances of 2.3 and 2.4 Å, the propensity of Ca^{2+} to coordinate carbonyl oxygens, and the octahedral coordination geometry.

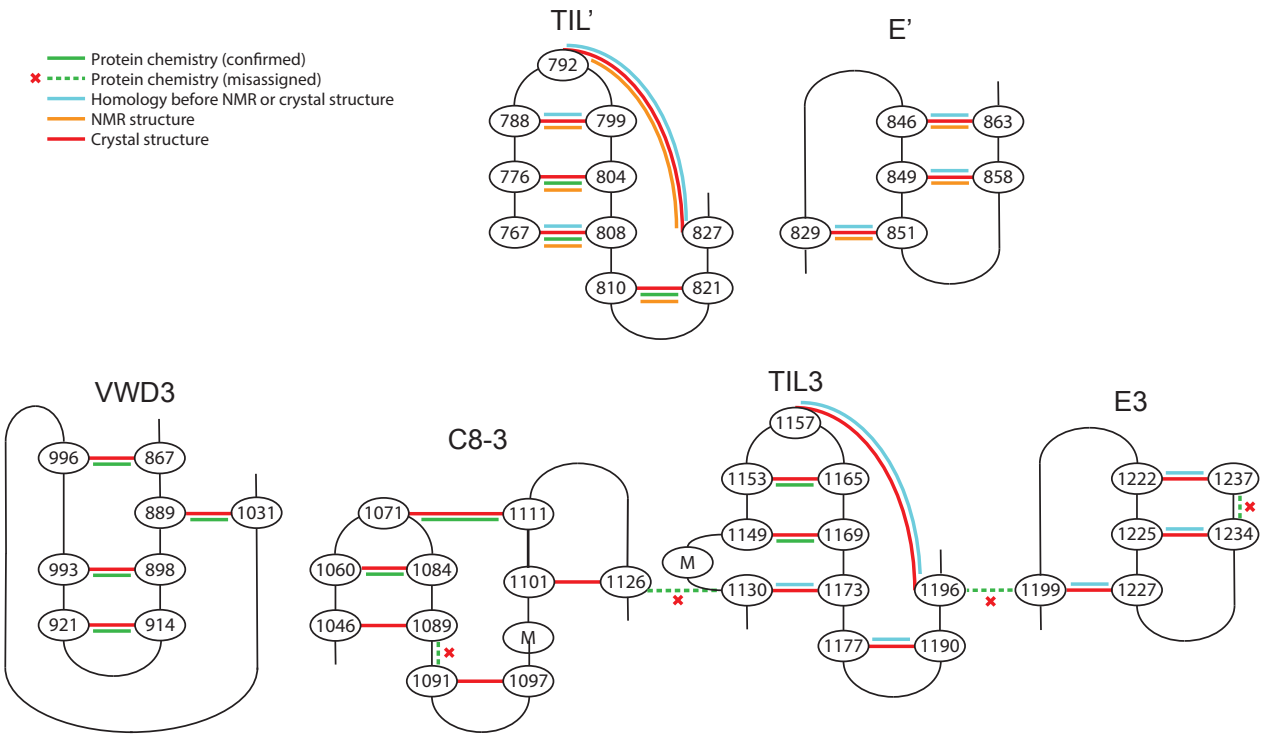

Supplemental Figure 4. Graphical representation of the disulfide bonds defined by different methods in the domains of D'D3. Green lines denote disulfide bonds that were determined by protein chemistry (*Marti, T., Rosselet, S. J., Titani, K., and Walsh, K. A. (1987) Identification of disulfide-bridged substructures within human von Willebrand factor. Biochemistry 26, 8099-8109*) and subsequently confirmed (solid lines) or found to be incorrect (dashed lines with red asterisks). Cyan lines show all disulfide bonds predicted by homology and loss or absence of pairs of cysteines (*Zhou, Y. F., Eng, E., Zhu, J., Lu, C., Walz, T., and Springer, T. A. (2012) Sequence and structure relationships within von Willebrand factor. Blood 120, 449-458*). Orange lines show disulfides found in the NMR structure of D' (*Shiltagh, N., Kirkpatrick, J., Cabrita, L. D., McKinnon, T. A., Thalassinos, K., Tuddenham, E. G., and Hansen, D. F. (2014) Solution structure of the major factor VIII binding region on von Willebrand factor. Blood 123, 4143-4151*). Red lines show disulfide bonds found here in the crystal structure.

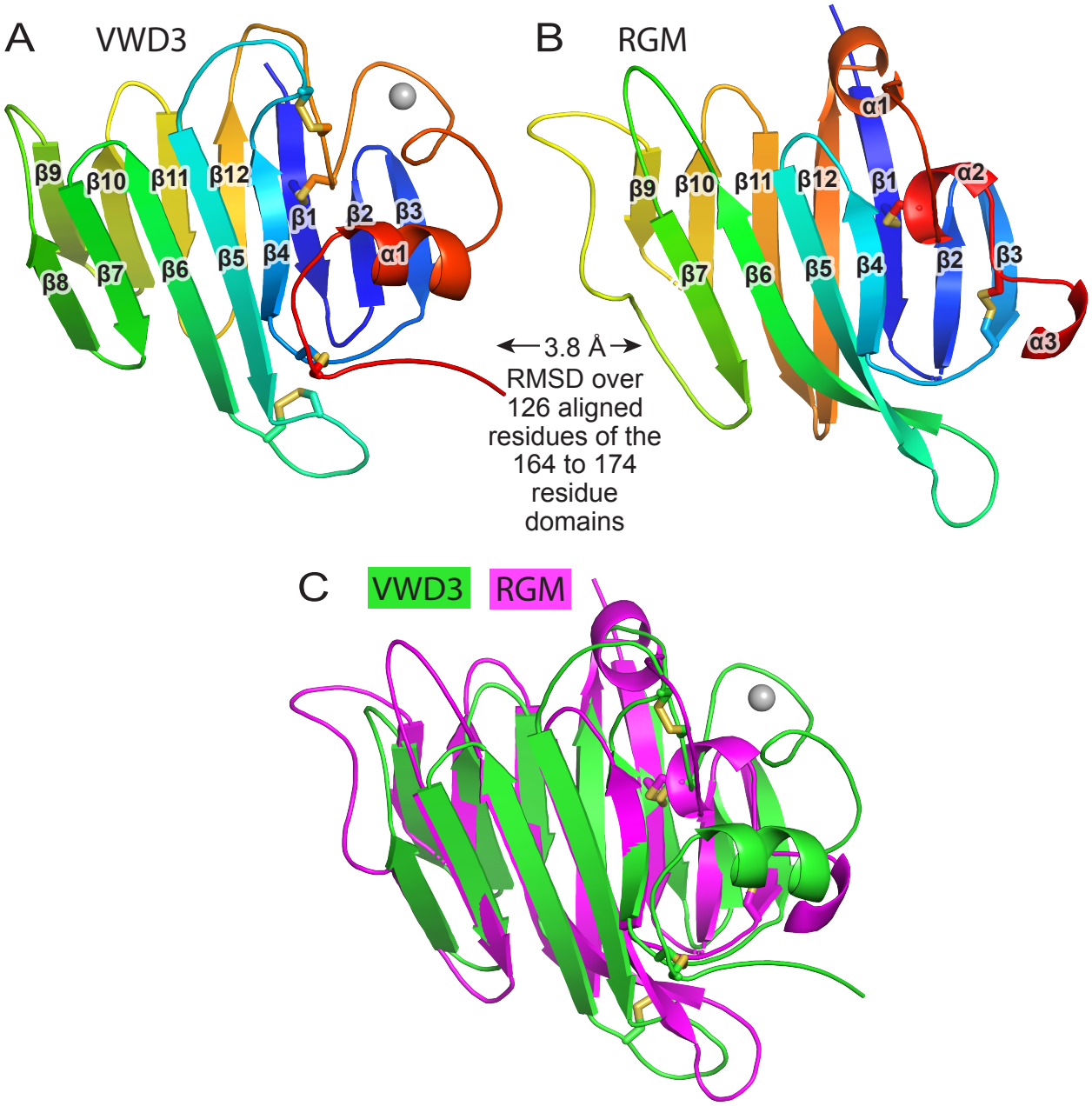

Supplemental Figure 5. Structural homology of the VWD domains in VWF D3 and repulsive guidance molecules (RGM). (A and B) Superimposed domains are shown in rainbow in identical orientations or (C) in different colors. Representations are as in Fig. 1. RGM domain is from PDB ID code 4BQ6. Superposition was with the Deep Align server (*Wang, S., Ma, J., Peng, J., and Xu, J. (2013) Protein structure alignment beyond spatial proximity. Sci. Rep. 3, 1448*).

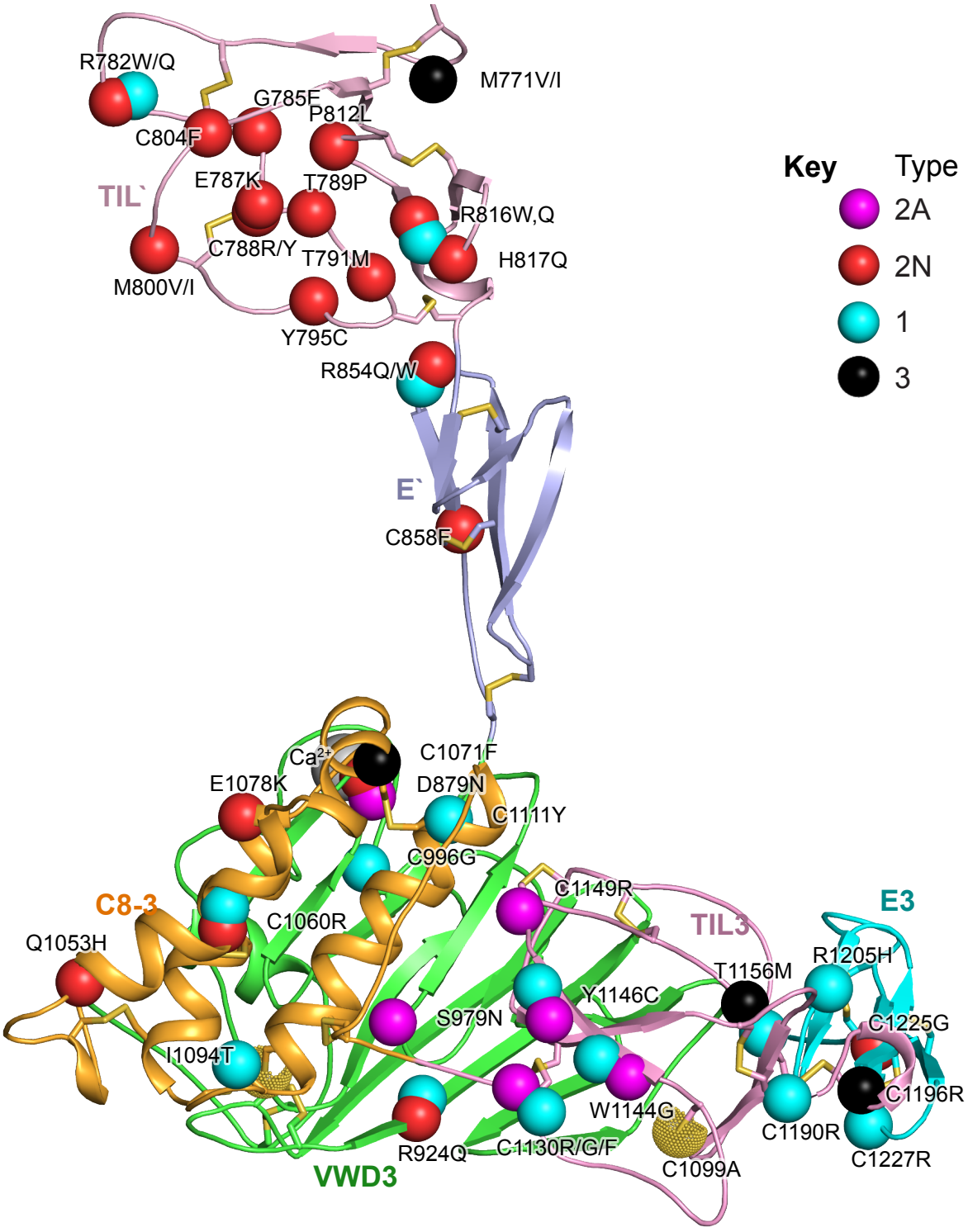

Supplemental Figure 6. Locations of VW disease mutations within D'D3 are shown as spheres at mutated residues. Each type of mutation is color coded in the key. When more than two disease types are reported for a residue, a sphere is shown for each disease type. To facilitate display, mutated residues are displayed with spheres on amino acid residue backbone atoms Cα (type 2N), C (type 1), and N (type 2A and 3, which currently have no overlapping residues). Mutations were taken on Aug.19, 2018 from the International Society for Hemostasis and Thrombosis Database. *Hampshire, D. J., and Goodeve, A. C. (2011) The International Society on Thrombosis and Haematosis von Willebrand disease database: an update. Semin. Thromb. Hemost. 37, 470-479.*

Supplemental Video 1. D'D3 structure. D'D3 is rotated. Figures prepared with PyMol show ribbon cartoon and disulfides and N-glycans with white carbons in stick, red oxygens, blue nitrogens, and yellow sulfurs. Ca^{2+} is shown as a silver sphere. A1099 and A1142 are modeled as cysteines using the one allowed rotameric position of the S atom, as discussed in Results. Dot surfaces around the S atom emphasize that there is room for it in the structure and that it is a model.

Supplemental Video 2. Structure around the buried cysteine residues required for D3 dimerization. A1099 and A1142 are shown as cysteines as described in the legend for Video 1, and sidechains of residues that bury the Cys sidechains are shown as stick. The movie zooms in to view the position of each mutated Cys residue, first residue 1099 in C8-3 and then residue 1142 in TIL3.